



AMS

American Meteorological Society

Supplemental Material

Journal of Climate

The Roles of Westward-Propagating Waves and the QBO in Limiting MJO Propagation

<https://doi.org/10.1175/JCLI-D-21-0691.1>

© Copyright 2022 American Meteorological Society (AMS)

For permission to reuse any portion of this work, please contact permissions@ametsoc.org. Any use of material in this work that is determined to be “fair use” under Section 107 of the U.S. Copyright Act (17 USC §107) or that satisfies the conditions specified in Section 108 of the U.S. Copyright Act (17 USC §108) does not require AMS’s permission. Republication, systematic reproduction, posting in electronic form, such as on a website or in a searchable database, or other uses of this material, except as exempted by the above statement, requires written permission or a license from AMS. All AMS journals and monograph publications are registered with the Copyright Clearance Center (<https://www.copyright.com>). Additional details are provided in the AMS Copyright Policy statement, available on the AMS website (<https://www.ametsoc.org/PUBSCopyrightPolicy>).

SI. 1. A Case Study of the Hindered Descending Branch NP MJO

For each type of MJO, 4 events are selected for further diagnosis to confirm that the mechanisms identified are present not only in composite analysis, but also in individual events. Namely, we confirm whether the WPWs and their ability to hinder the descending motion of NP MJO, but not EP MJO can be identified in these events. The vertical circulation of NP MJO cases (Fig.S1 and Fig.S3) shows a well-organized descending branch around day -5, and the active convection of WPWs over the Pacific weakens the descending branch from day 0. As a result, the meridional moisture advection for the selected NP MJO cases is insufficient to support their propagation across the MC (Fig.S2 and Fig.S4). In contrast, EP MJO cases are coupled with strong descending branches during their propagation across the MC around day 0 (Fig.S5 and Fig.S7), providing sufficient meridional moisture advection over the southern sea surface of the MC (Fig.S6 and Fig.S8). Note that for one stand case (20111221) and one jump case (19890226), the active convection of the WPWs is already evident and it impacts the MJO descending branch around day -5. Therefore, the descending branches of these two MJO cases are weak in Fig.S1 and Fig.S3.

Stand Cases

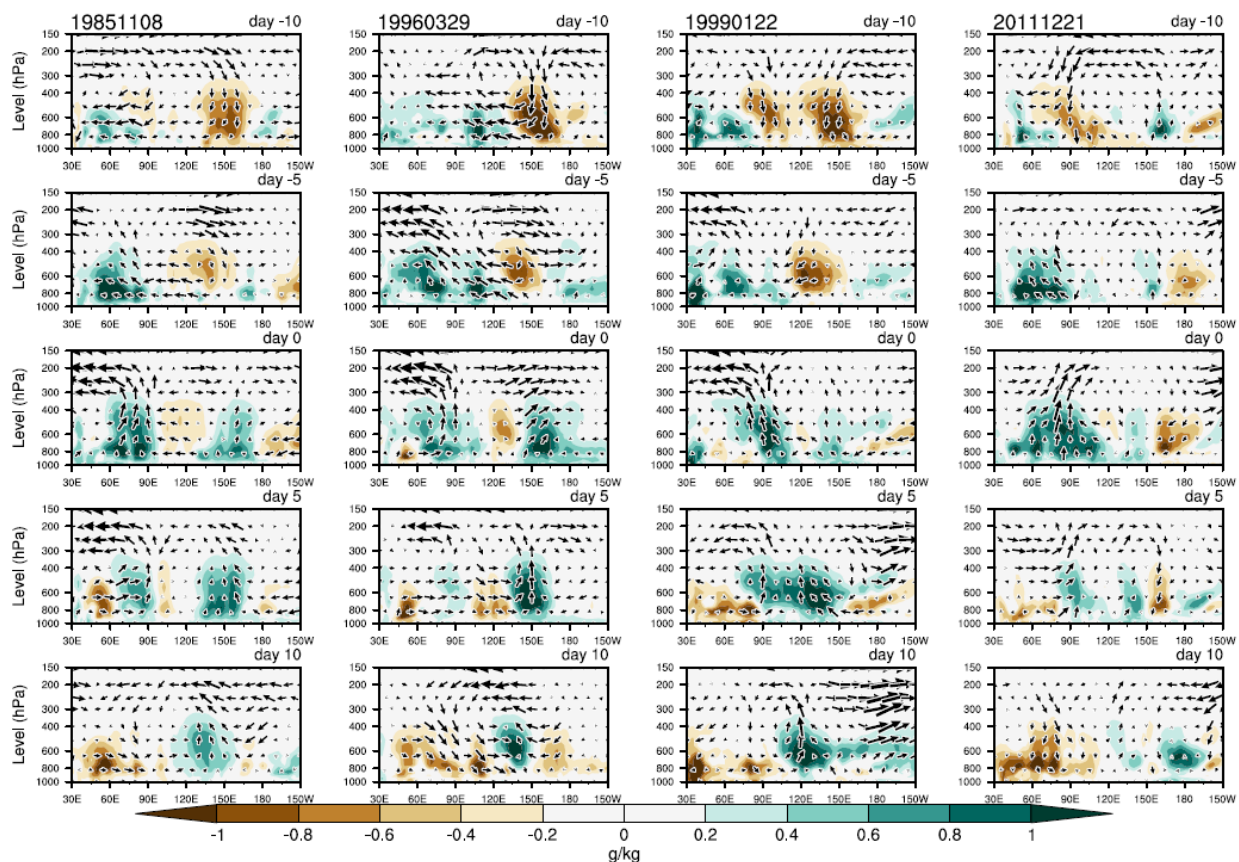


Fig. S1. Vertical sections (10°S - 10°N) of intraseasonal (20-70-filtered) specific humidity (shading) and vertical circulation (vectors) from day -10 to day 10 for 4 stand MJO cases. The reference day (day 0) is labeled on top of each column.

Stand Cases

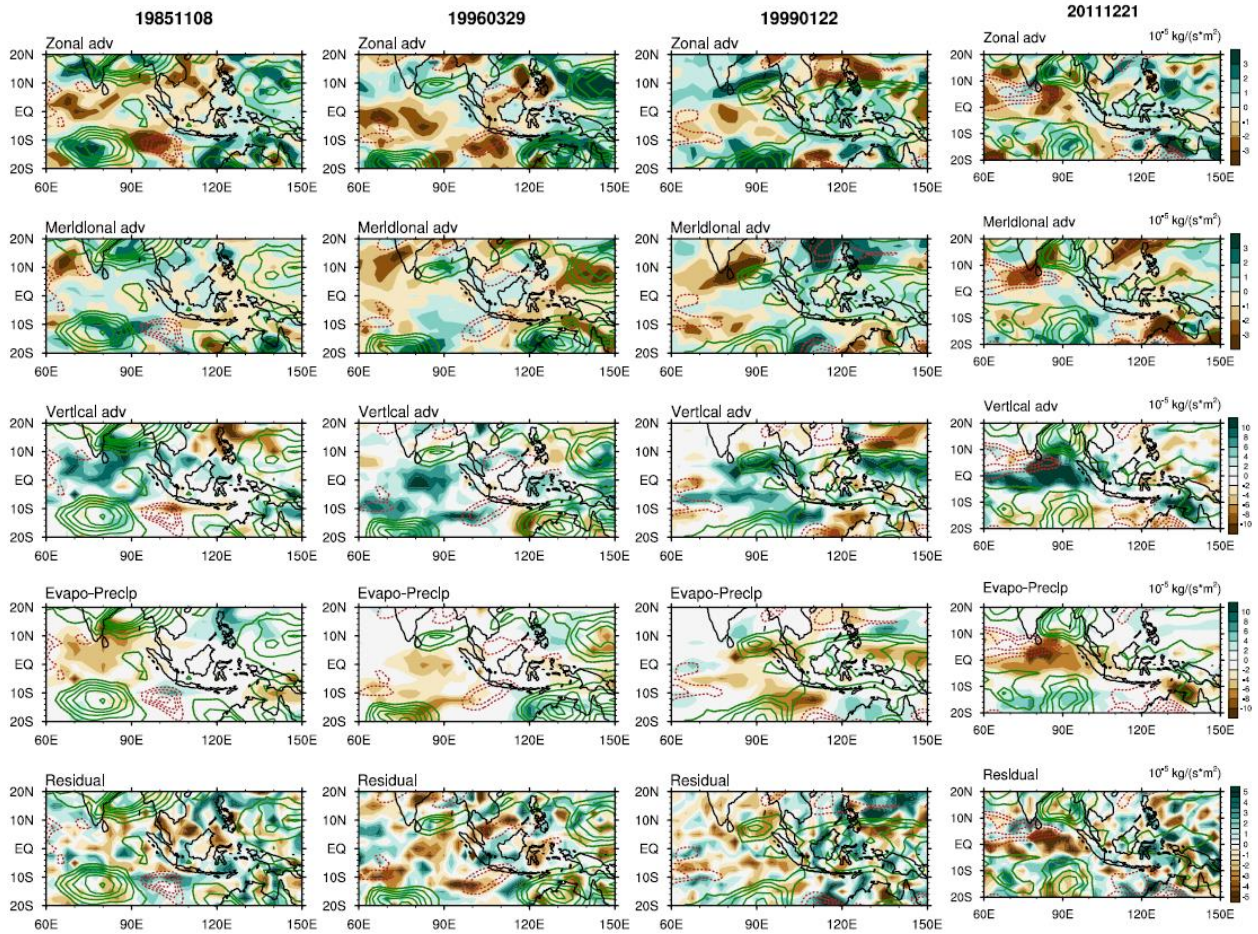


Fig. S2. Column-integrated (surface to 100hPa) moisture tendency (lines) and the right-hand-side term (shadings) maps for the same 4 stand MJO cases as in Fig.S1. Positive moisture tendencies are represented by solid green lines and negative tendencies are represented by red dotted lines with an interval of $0.5 \times 10^{-5} \text{ kg}/(\text{m}^2 \cdot \text{s})$.

Jump Cases

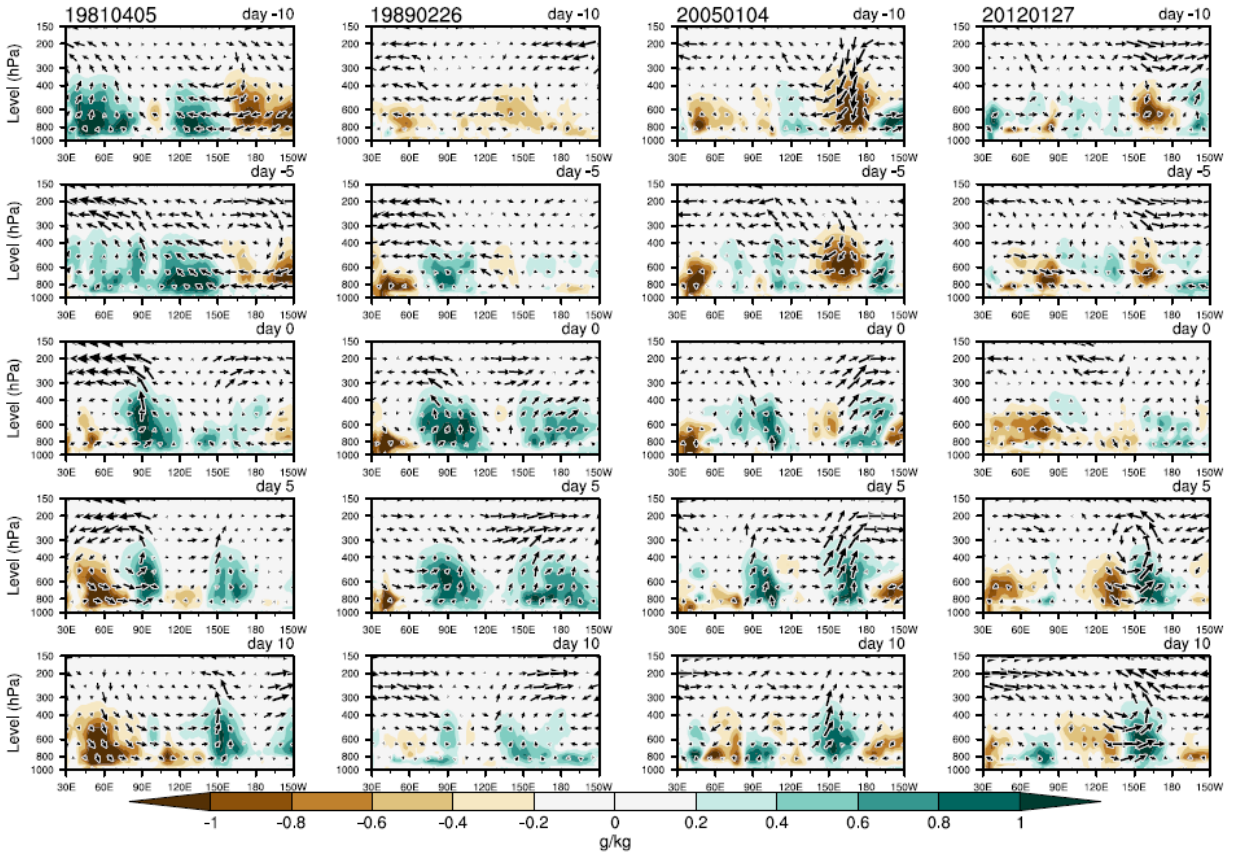


Fig. S3. Same as in Fig.S1, but for 4 jump MJO cases.

Jump Cases

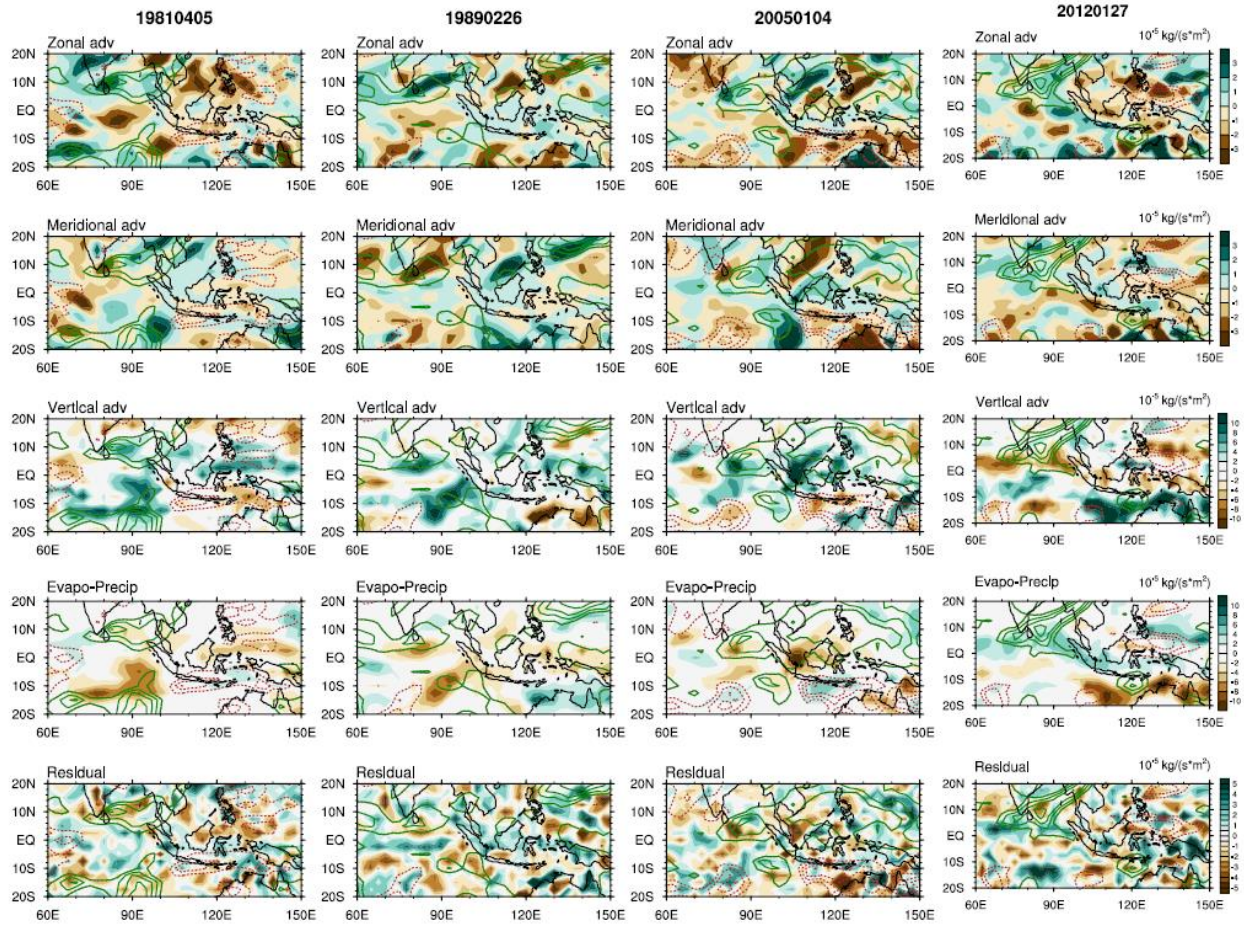


Fig. S4. Same as in Fig.S2, but for 4 jump MJO cases.

Slow Cases

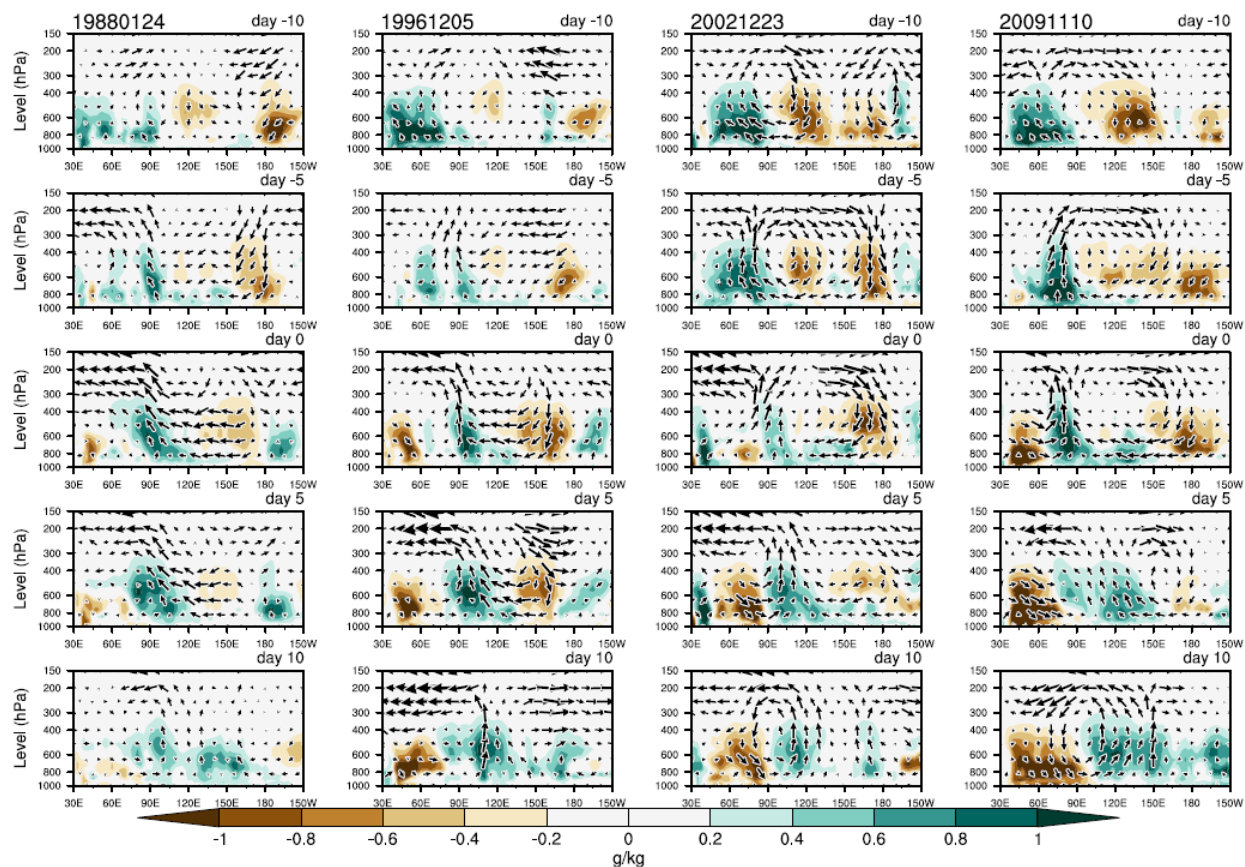


Fig. S5. Same as in Fig.S1, but for 4 slow MJO cases.

Slow Cases

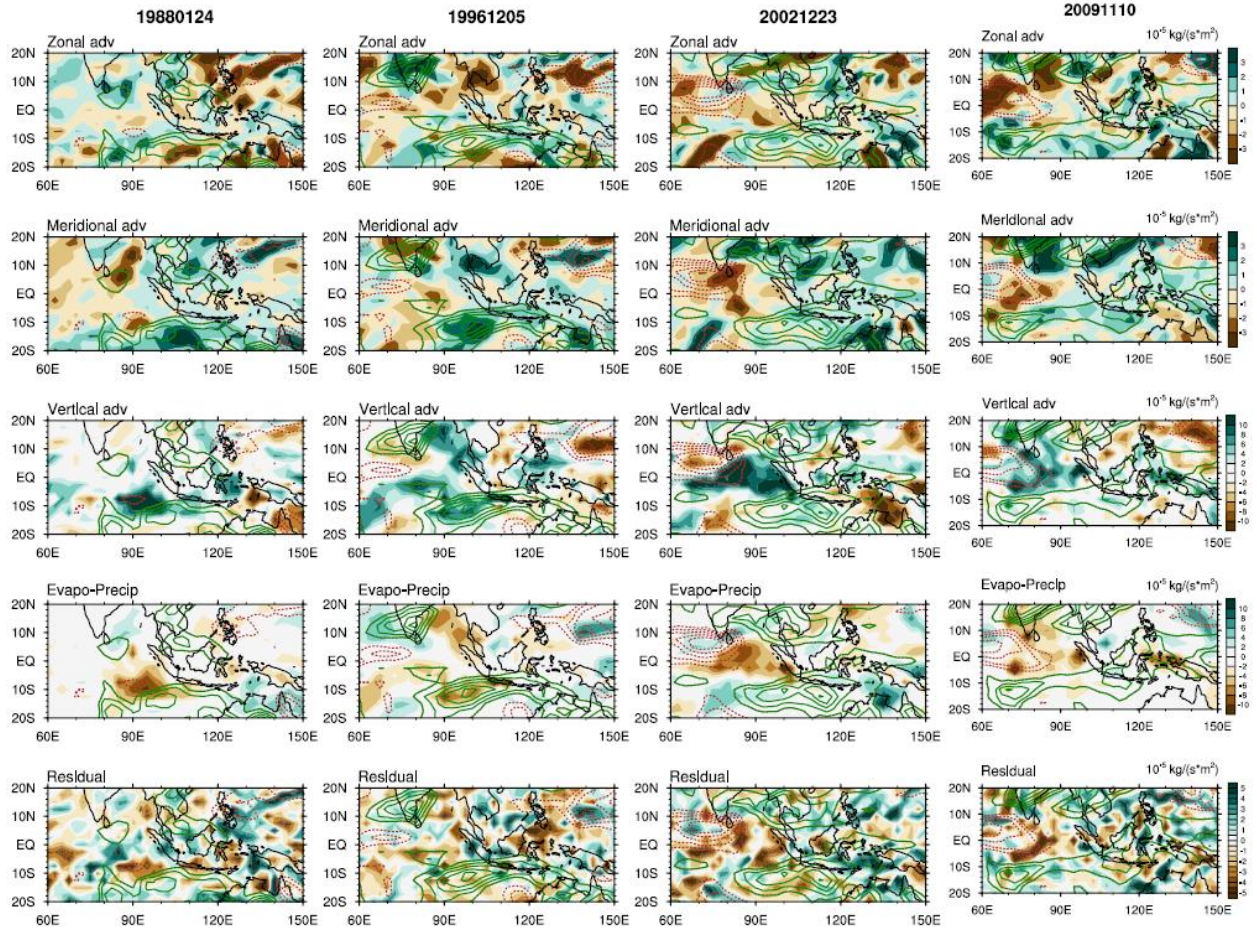


Fig. S6. Same as in Fig.S2, but for 4 slow MJO cases.

Fast Cases

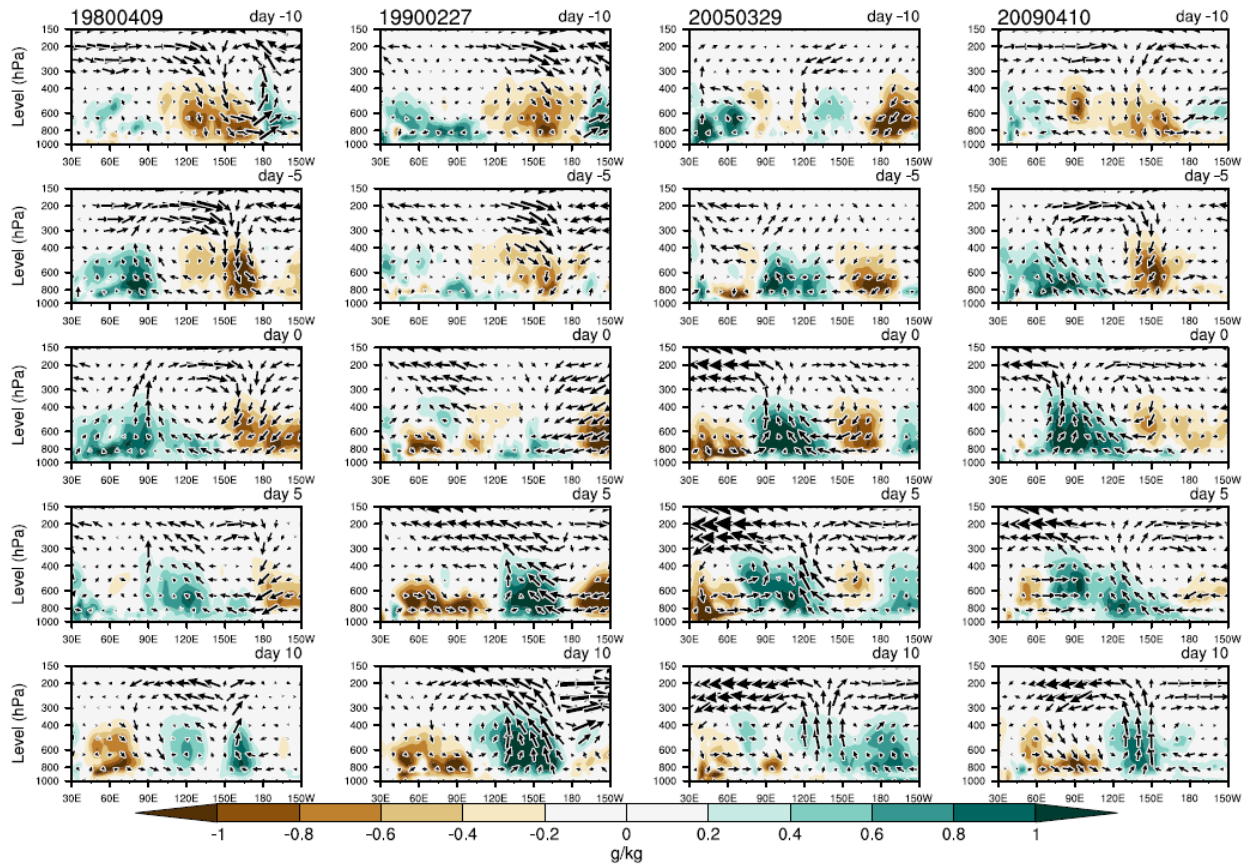


Fig. S7. Same as in Fig.S1, but for 4 fast MJO cases.

Fast Cases

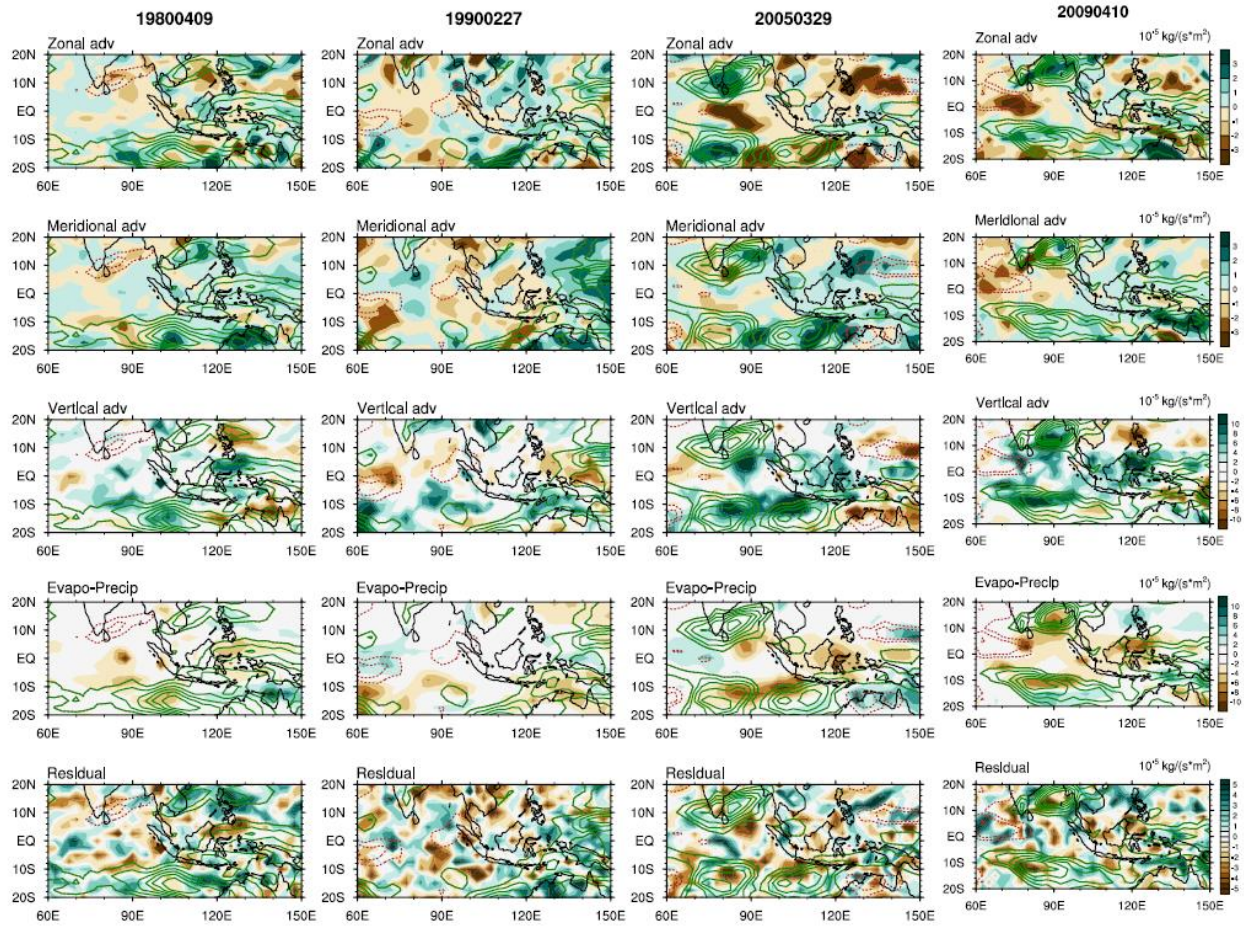


Fig. S8. Same as in Fig.S2, but for 4 fast MJO cases.

SI.2. Influences of the Intraseasonal and Seasonal-mean Moisture Field

The intraseasonal dry anomalies induced by the WPW over the northeastern MC are important for jump MJO events as shown in Fig.S9. The intraseasonal dry anomalies are collocated with local seasonal-mean northeasterlies. Therefore, they are advected into the MC by the seasonal-mean wind and lead to an overall drying anomaly over the MC for jump MJO.

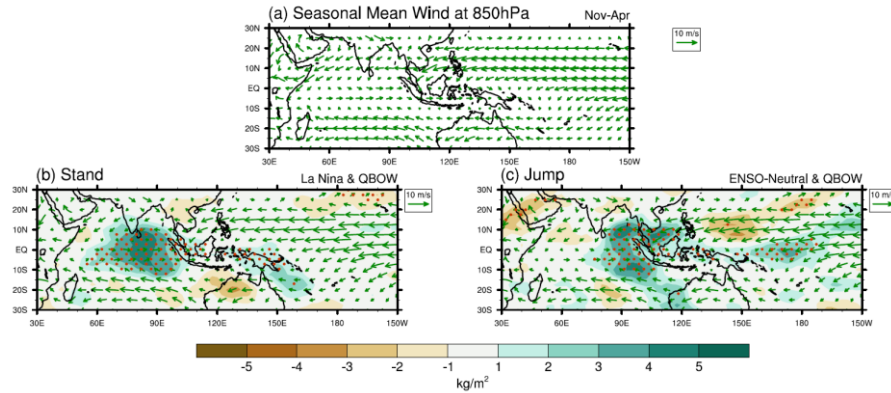


Fig. S9. Composited maps of the intraseasonal column-integrated specific humidity anomalies (shading) and the 3-month-mean wind at 850hPa (vectors) for (b) stand and (c) jump MJO. The reference seasonal-mean wind at 850hPa in the boreal winter season is given in (a). The intraseasonal moisture anomalies exceeding 95% confidence level are stippled.

The background seasonal-mean moisture field is different among MJO types as in Fig.S10. The stand and fast MJO have significantly different seasonal mean moisture background. For stand MJO, there are dry anomalies over the central-eastern Pacific and the southern Indian Ocean while the northern hemisphere shows an overall wetting centered at the South China Sea. For fast MJO, the seasonal-mean moisture background shows some wetting over the central-eastern Pacific and some drying over the southern MC and northern Australia. Such contrast between the seasonal-mean moisture background is probably related to different ENSO states for stand and fast MJO since ENSO can impact the SSTA pattern and therefore the moisture field.

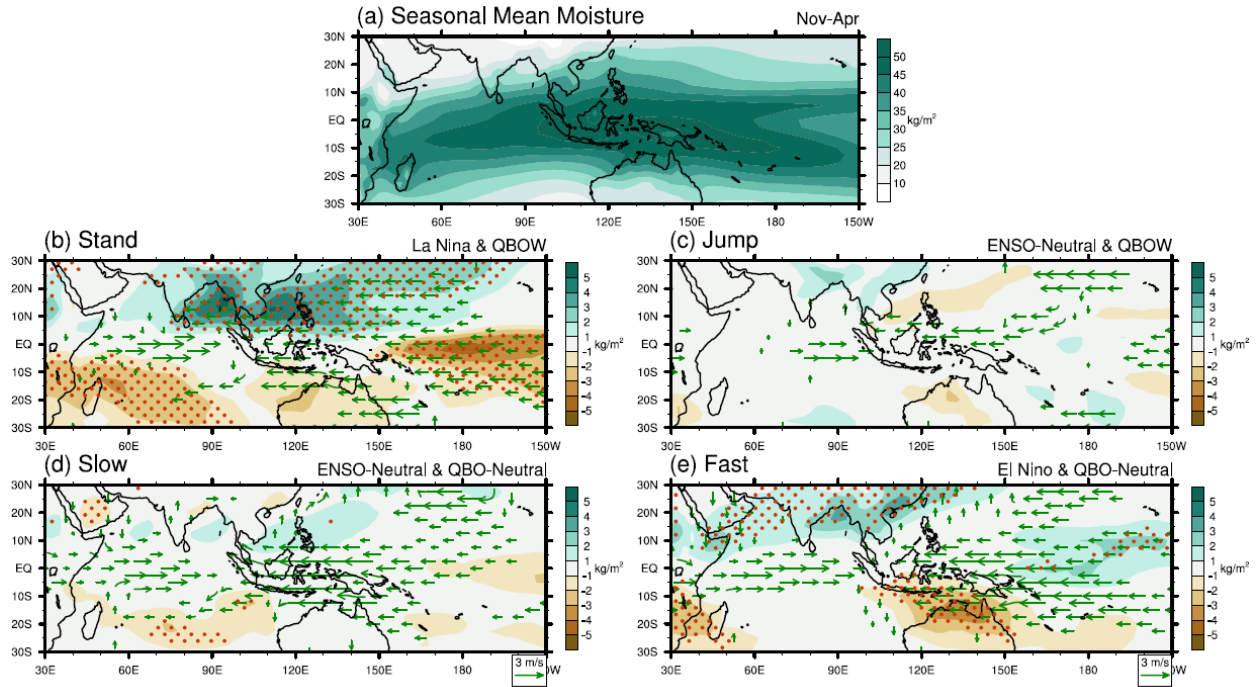


Fig. S10. (a) The boreal winter seasonal-mean moisture (column-integrated specific humidity) field, and (b)-(e) composited maps of the bias of 3-month-mean moisture field from the reference boreal winter seasonal mean (shading) and the intraseasonal wind anomalies at 850hPa (vectors) for four MJO types. The preferred ENSO and QBO phases are labeled on the top right of each panel. Only the intraseasonal wind anomalies exceeding 95% confidence level are drawn. The biases in 3-month-mean moisture exceeding 95% confidence level are stippled.